EBioMedicine 000 (2019) 1–13

Contents lists available at ScienceDirect

EBioMedicine

journal homepage: www.elsevier.com/locate/ebiom

EBioMedicine
Published by THE LANCET

Research paper

H19 promote calcium oxalate nephrocalcinosis-induced renal tubular epithelial cell injury via a ceRNA pathway

Haoran Liu[a,b], Tao Ye[a], Xiaoqi Yang[a], Jianhe Liu[b], Kehua Jiang[a,c], Hongyan Lu[a,d], Ding Xia[a], Ejun Peng[a], Zhiqiang Chen[a], Fa Sun[c], Kun Tang[a,*], Zhangqun Ye[a]

[a] Department of Urology, Tong Hospital, Tongji Medical College, Huazhong University of Science and Technology, Wuhan 430030, PR China
[b] Department of Urology, The Second Affiliated Hospital of Kunming Medical University, Kunming, 650000, PR China
[c] Department of Urology, Guizhou Provincial People's Hospital, Guiyang, 550000, PR China
[d] Department of Urology, The Third Affiliated Hospital of Chongqing Medical University, Chongqing, 409912, PR China

ARTICLE INFO

Article History:
Received 22 July 2019
Revised 30 October 2019
Accepted 31 October 2019
Available online xxx

Keywords:
H19
calcium oxalate
tubular epithelial cell injury
HMGB1
ceRNA

ABSTRACT

Background: Intrarenal calcium oxalate (CaOx) crystals induce inflammation and kidney tubular cell injury, which are processes that involve TLR4/NF-κB signalling. A recent genome-wide gene expression profile analysis of Randall's plaques in CaOx stone patients revealed that the expression of the long noncoding RNA H19 was significantly upregulated. However, to date, its role in kidney CaOx stones has not been reported.
Method: A Gene Expression Omnibus (GEO) dataset was utilized to analyse gene expression profiles. Luciferase reporter, Western blotting, qRT-PCR, immunofluorescence staining and reactive oxygen species (ROS) assays were employed to study the molecular mechanism of HMGB1/TLR4/NF-κB regulation by H19 and miR-216b. *In vitro* and *in vivo* assays were performed to further confirm the proinflammatory and prooxidative stress effects.
Finding: H19 expression was significantly increased and positively correlated with the expression levels of HMGB1, TLR4 and NF-κB in Randall's plaques and glyoxylate-induced CaOx nephrocalcinosis mouse models. H19 interacted with miR-216b and suppressed its expression. Additionally, miR-216b inhibited HMGB1 expression by directly binding its 3′-untranslated region. Moreover, H19 downregulation inhibited HMGB1, TLR4 and NF-κB expression and suppressed CaOx nephrocalcinosis-induced renal tubular epithelial cell injury, NADPH oxidase, and oxidative stress *in vivo* and *in vitro*. Interestingly, miR-216b inhibition partially reversed the inhibitory effect of H19 knockdown on HMGB1 expression.
Interpretation: We determined that H19 might serve as a facilitator in the process of CaOx nephrocalcinosis-induced oxidative stress and renal tubular epithelial cell injury, and we revealed that the interaction between H19 and miR-216b could exert its effect via the HMGB1/TLR4/NF-κB pathway.
Funding: This work was supported by the National Nature Science Foundation of China (Nos. 8196030190, 8190033175, 81370805, 81470935, 81900645, 81500534, and 81602236).
© 2019 Published by Elsevier B.V. This is an open access article under the CC BY-NC-ND license. (http://creativecommons.org/licenses/by-nc-nd/4.0/)

Research in context

Evidence before this study

Asymptomatic calcium oxalate (CaOx) nephrocalcinosis can lead to chronic nephropathy and subsequent renal failure. Intrarenal CaOx crystals trigger neutrophil recruitment, induce cytokine expression and promote renal tubular cell injury. The HMGB1/TLR4/NF-kB pathway is critical for immune activation and subsequent inflammatory responses to tissue injury and is involved in the pathogenesis of cellular injuries in the kidney. A recent genome-wide gene expression profile analysis of Randall's plaques in CaOx stone patients demonstrated that lncRNA H19 expression was significantly upregulated. Emerging evidence has shown that H19 is involved in inflammatory regulation and induces tissue injury. However, its regulatory function in CaOx nephrocalcinosis remains largely unknown.

Added value of this study

H19 and HMGB1 were overexpressed while miR-216b was suppressed in glyoxylate-induced CaOx nephrocalcinosis mouse model, and H19 negatively regulated miR-216b expression in COM crystal

* Corresponding author at: Dr. Kun Tang, Department of Urology, Tongji Hospital, Tongji Medical College, Huazhong University of Science and Technology, Wuhan 430030, PR China.
E-mail address: tangsk1990@163.com (K. Tang).

https://doi.org/10.1016/j.ebiom.2019.10.059
2352-3964/© 2019 Published by Elsevier B.V. This is an open access article under the CC BY-NC-ND license. (http://creativecommons.org/licenses/by-nc-nd/4.0/)

co-cultured renal tubular epithelial cells. H19 activation increased HMGB1, TLR4 and NF-κB expression, promoted renal tubular epithelial cell injury and further aggravated CaOx crystal deposition *in vivo* and *in vitro*. Moreover, miR-216b directly inhibited HMGB1 expression by directly binding its 3′-untranslated region. In addition, the inhibition of miR-216b can partially reverse the inhibitory effect of H19 knockdown on HMGB1 expression.

Implications of all the available evidence

We found that H19 and miR-216b play crucial roles in CaOx nephrocalcinosis-induced renal tubular epithelial cell injury and glyoxylate-induced kidney CaOx crystal deposition. We also revealed the mechanism by which the H19 sponging of miR-216b exerts its effect by activating the HMGB1/TLR4/NF-kB pathway. Our study provides new insight into the novel mechanism by which H19 regulates the HMGB1/TLR4/NF-kB pathway by competitively binding miR-216b, suggesting that H19 might be a potent therapeutic target in CaOx nephrocalcinosis disease.

1. Introduction

Kidney stone disease affects approximately 9% of adults worldwide during their lifetime, and this number continues to increase [1,2]. Calcium oxalate (CaOx), which is the major component of kidney stones, can lead to increased intrarenal inflammation and kidney tubular cell necroptosis and consequentially induce more CaOx crystal adhension [3]. Previous studies have identified high-mobility group box 1 (HMGB1) as an important damage-associated molecular pattern molecule [4]. HMGB1 binds toll-like receptor 4 (TLR4), which leads to the activation of nuclear factor kappa B (NF-κB) and increases in the transcription and expression of several proinflammatory cytokines and chemokines [5]. The HMGB1/TLR4/NF-κB pathway is critical for immune activation and subsequent inflammatory responses to tissue injury and is involved in the pathogenesis of cellular injuries in various organs, *e.g.*, the liver, lung, brain, and kidney [5–7]. Wang et al. found that urinary HMGB1 was increased in patients with calcium nephrolithiasis and that hypercalciuria might affect reactive oxygen species (ROS) that stimulate HMGB1 production *in vivo* [8].

As one of the first identified and best characterized long noncoding RNAs (lncRNAs), H19 has been recognized for its broad spectrum of biological functions in many physiological and pathological processes [9]. Emerging evidence has shown that H19 is involved in inflammatory regulation and induces tissue injury [10–12]. However, its regulatory function in CaOx nephrocalcinosis remains largely unknown. A recent genome-wide gene expression profile analysis of Randall's plaques in CaOx stone patients demonstrated that lncRNA H19 expression was significantly upregulated [13], indicating that H19 plays a relevant regulatory role in CaOx nephrocalcinosis.

In our study, we demonstrated that the H19/miR-216b interaction is involved in tubular epithelial cell injury in a glyoxylate-induced CaOx nephrocalcinosis mouse model and highlighted the underlying mechanisms by which H19 sponges miR-216b-3p to promote CaOx nephrocalcinosis-induced renal tubular epithelial cell injury via HMGB1/TLR4/NF-κB pathway activation.

2. Materials and methods

2.1. Cell culture

The normal human proximal tubular epithelial cell line HK-2 was purchased from the American Type Culture Collection (ATCC) and maintained in dulbecco's modified eagle'smedium (DMEM) supplemented with 10% FBS and 1% penicillin/streptomycin in a humidified atmosphere of 5% CO2.

2.2. Reagents and transfection

To over expression of H19, lentivirus H19 and negative control were synthesized and purchased from Vigene Biosciences (Jinan, Shandong, China). Lentivirus were diluted with 200 μL Opti-MEM medium (Gibco, UK) at 10^7 transduction units (TU)/mL containing Polybrene (5 mg/mL) and incubated with cells for 2 h. The medium was then replaced by DMEM and cultured for 24 h. To knock down H19, a prevalidated siRNA against H19 was synthesized by Vigene Biosciences (si-H19: 5′-GCCTTCAAGCATTCCATTA-3′). Chemosynthetic miRNA oligonucleotides (miR-216b mimics, miR-216b inhibitor, and negative control) were purchased from Ribo Biotech (Guangzhou, China). 50 nM si-H19 or 50 nM miR-216b mimics or 100 nM miR-216b inhibitor were added into 200 μL Opti-MEM medium with 5 μL Lipofectamine 3000 (Invitrogen, CA, USA). The mixed medium was incubated for 15 min then add to cells for culture.

2.3. Animal procedures

All experimental procedures followed the rules of the National Institutes of Health Guide for the Care and Use of Laboratory Animals. C57BL/6 J male mice (6–8 weeks old) were used in the experiments. To establish the CaOx nephrocalcinosis model, each C57BL/6 J male mouse received either intraperitoneal vehicle (saline) or glyoxylate (glyoxylic acid, GA) (75 mg/kg, 200 μl) every day for two weeks. In the H19 intervention groups, 6-week-old mice were placed in a restraint that positioned the mouse tail in a lighted, heated groove. The tail was swabbed with alcohol and then injected intravenously with 100 μl recombinant (rAAV)-H19 or rAAV-vector as a negative control (synthesized by Vigene Biosciences, Shandong, China). For the rAAV-H19 packaging, a rAAV 2/9-CMV-eGFP vector was used (3×10^{12} viral genome rAAV). A correct injection was verified by noting blanching of the vein. Two weeks after AAV injection, immunofluorescence was performed to confirm that H19 was overexpressed in the mouse kidneys (Supplementary Fig. S1). To explore the effects of HMGB1 on CaOx crystal formation in kidney, 3 mg/kg HMGB1-neutralizing Ab (Shino-test, Kanagawa, Japan) and paired control IgG were treated intraperitoneally to recipient mice on day 1, 4, 7, 10, 13 [14,15]. To evaluate the effect of miR-216b, mice received miR-216b long-lasting agonist (Ribo Biotech) on day 1 and 8 as a dose of 80 mg/kg (200 μL) body weight through tail vain. After two weeks, the mice were sacrificed and subjected to laparotomy for further assessment. All animal experiments were approved by the Ethics Committee of Tongji Hospital, Huazhong University of Science and Technology.

2.4. Detection of kidney CaOx crystals

CaOx crystal deposition in the kidneys was determined using Pizzolato staining and polarized light optical microphotography (Zeiss, Oberkochen, Germany) and then quantified as the percent area of crystal deposition per kidney section with Image-Pro-Plus (Media Cybernetics, Inc., Bethesda, MD).

2.5. Tubular injury score

Kidney tissue sections were stained with periodic acid-Schiff (PAS) to assess tubular injury. Scoring was performed by grading tubular necrosis, epithelial cell apoptosis, intraluminal cast formation and brush border loss in 10 randomly chosen, nonoverlapping microscopic fields (100 ×). The tubular lesions were graded on a scale from 0 to 5 as follows: 0 (none), 1 (≤ 10%), 2 (11–25%), 3 (26–45%), 4 (46–75%), and 5 (≥ 76%).

Please cite this article as: H. Liu et al., H19 promote calcium oxalate nephrocalcinosis-induced renal tubular epithelial cell injury via a ceRNA pathway, EBioMedicine (2019), https://doi.org/10.1016/j.ebiom.2019.10.059

2.6. Real-time PCR

Total RNA was isolated from cultured cells with TRIzol reagent (Invitrogen, CA) following the manufacturer's instructions. Then, the total RNA was converted into cDNA using a Prime-Script One Step RT-PCR Kit (TAKARA, Japan). Real-time PCR was performed to determine mRNA expression levels using a Bio-Rad CFX96 system with SYBR Green. The quantitative detection of mature miRNA was conducted with an All-in-One miRNA qRT-PCR Detection Kit (GeneCopoeia). cDNA was obtained by reverse transcription of the total RNA. All-in-One miRNA primers were used in the RT-qPCR analysis to detect specific miRNAs. Relative RNA expression of gene or lncRNA was calculated using the $2^{-\Delta\Delta Ct}$ method by normalizing to β-actin expression. The quantification of microRNA expression, U6 was used as an endogenous nor-malizer. The primers used in our research are presented in Supplementary Table S1.

2.7. Intracellular ROS detection using flow cytometry

HK-2 cells were cultured in six-well plates and exposed to 100 μg/mL calcium oxalate monohydrate (COM, Sigma-Aldrich, C0350000) for 2 h [16]. Then, the cells were treated with 2,7-dichlorofluorescein diacetate (DCFH-DA) for 30 min, collected, and resuspended in PBS. Finally, intracellular ROS production was determined using flow cytometry with excitation and emission at 485 and 538 nm, respectively (BD Bioscience, USA).

2.8. Lactate dehydrogenase (LDH), malondialdehyde (MDA), H2O2, and superoxide dismutase (SOD) level determination

HK-2 cells were seeded into 96-well plates and cultured overnight with 100 μg/ml COM. After centrifugation, the levels of LDH released in the supernatants were determined using an LDH Assay Kit (Beyotime Biotech, China). Lipid peroxidation was measured as the MDA content and determined with an MDA Kit (Beyotime Biotech, China). The H_2O_2 concentrations in the culture medium were measured using an H_2O_2 kit (Beyotime Biotech, China), and the results were determined at 595 nm. SOD activity was determined by the method proposed by Misra and Firidovich (1972). The SOD levels were determined spectrophotometrically at 480 nm and expressed as a % of the control.

2.9. Western blot analysis

Protein extracts were separated by 10% SDS-PAGE, electrophoretically transferred to PVDF membranes, and incubated overnight at 4 °C with primary antibodies, including HMGB1 (25 kD, 1:1000, Boster, China, BM3965), TLR4 (96 kDa, 1:1000, Boster, China, BA1717), NF-kB (65 kDa, 1:1000, Boster, China BM3940), p-NF-kB (65 kDa, 1:1000, Servicebio, China, GB11142-1), and β-Actin (43 kDa, 1:500, Boster, China, BM01263-2). Then, the membrane strips were incubated with the appropriate horseradish peroxidase-conjugated secondary antibodies. The protein bands were visualized using an ECL kit (Millipore, USA) with a chemiDoc XRS (Bio-Rad) instrument. Image J software was used to calculate the relative density of proteins.

2.10. Luciferase reporter assay

To construct luciferase reporter plasmids, H19 and the 3′-untranslated region (UTR) of HMGB1 containing the predicted miR-216b binding site and the mutated site were inserted into a psiCHECK-2 vector (Promega, Madison, WI, USA). Then, the constructed vectors and chemically synthesized miR-216b mimics, inhibitor or negative controls were cotransfected into HK-2 cells using Lipofectamine 3000 (Invitrogen, Carlsbad, CA, USA). Forty-eight hours after transfection, luciferase activity was measured using a Dual-Luciferase Reporter Assay System (Promega, Madison, WI, USA). Relative protein levels are expressed as Renilla luciferase activity normalized to that of firefly luciferase.

2.11. Immunohistochemistry (IHC)

Mouse kidney tissues were formalin-fixed, paraffin-embedded, sectioned, and stained with haematoxylin and eosin (H&E) following standard histopathological techniques. For IHC, sections were incubated overnight at 4 °C with anti-HMGB1, anti-TLR4, anti-NF-kB, anti-SOD2 (Boster, China, BM4813) and anti-NOX2 (Boster, China, BA2811) antibodies and then detected using an Envision HRP Polymer System (Boster, China). All images were acquired by a high-throughput Leica SCN400 scanner. Image J software was used to calculate the relative expression of gene.

2.12. Flow cytometry analysis of necrosis

HK-2 cells were cultured on 6-well plates (2.5×10^5 cells/well). Cells were harvested with COM (100 μg/mL) for 24 h, stained with an Annexin V-FITC and PI Apoptosis Detection Kit (eBioscienc, San Diego, USA), and then evaluated by flow cytometry (BD Biosciences, Bedford, MD, USA). The experiments were repeated three times.

2.13. Statistical analysis

The measurement data are presented as the mean ± SD. Statistically significant differences between the control group and treated groups were determined by Student's *t*-test or one-way analysis of variance (ANOVA) carried out with GraphPad Prism 5.0. To analyse the correlation between genes, Pearson's correlation test was applied. *P*-values <0.05 were considered statistically significant.

3. Results

3.1. H19 and HMGB1 expression were significantly increased in the CaOx nephrocalcinosis mouse model

We searched the Gene Expression Omnibus (GEO) database for gene expression profiles and found one available GEO dataset (GSE73680) from a recent genome-wide gene expression profile analysis of Randall's plaques in 29 CaOx stone patients and 6 healthy controls [13]. The hierarchical clustering and heatmap analysis revealed that H19 was significantly upregulated, including in Randall's plaques from the CaOx stone patients (Fig. 1a). Next, we established a glyoxylate-induced kidney CaOx nephrocalcinosis mouse model *in vivo*. Polarized light optical microphotography and Pizzolato staining were performed to confirm the increased CaOx crystal deposition in the kidney (Fig. 1b). PAS staining further confirmed that CaOx nephrocalcinosis promoted renal injury (Fig. 1b). Strong IHC staining for HMGB1, TLR4 and NF-kB was observed in the kidneys of the CaOx mice (Fig. 1b). Additionally, we found that the mRNA levels of H19, HMGB1, TLR4 and NF-kB were significantly increased in the glyoxylate-induced CaOx nephrocalcinosis mouse kidney samples (Fig. 1c). Then, we examined their relationship by performing a Pearson correlation coefficient analysis. H19 expression was positively correlated with HMGB1, TLR4 and NF-kB expression (Fig. 1d-f). Furthermore, qRT-PCR analysis showed significant downregulation of H19, HMGB1, TLR4 and NF-kB expression in COM crystal-treated HK-2 cells (Fig. 1g). These data indicate that H19 and HMGB1 expression were remarkably increased in kidney CaOx crystal-treated cell lines and mouse models and that H19 and HMGB1 were positively correlated.

3.2. H19 facilitated CaOx nephrocalcinosis-induced renal tubular epithelial cell injury in vivo

To explore the effect of H19 on CaOx nephrocalcinosis-induced renal tubular epithelial cell injury, we first injected rAAV-H19 or rAAV-vector through the tail vein. Two weeks postinjection, these mice received an intraperitoneal glyoxylate injection for 1 week to establish the CaOx

Please cite this article as: H. Liu et al., H19 promote calcium oxalate nephrocalcinosis-induced renal tubular epithelial cell injury via a ceRNA pathway, EBioMedicine (2019), https://doi.org/10.1016/j.ebiom.2019.10.059

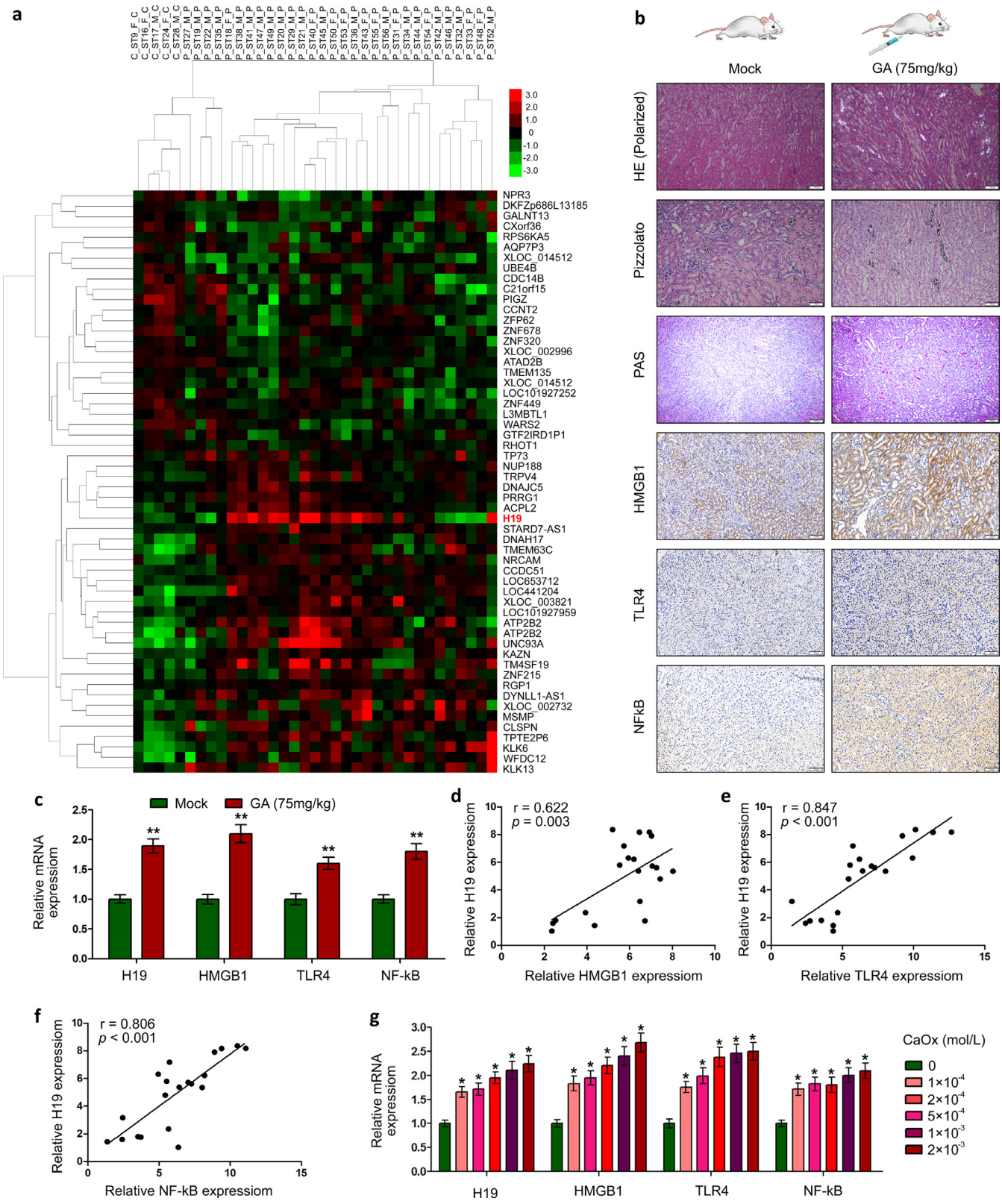

Fig. 1. H19 and HMGB1 expression was significantly increased in the CaOx nephrocalcinosis mouse model. (a) Hierarchical clustering and heatmap analysis of GSE73680 from a recent genome-wide gene expression profile analysis of Randall's plaques from 29 CaOx stone patients and 6 healthy controls. (b) A glyoxylate-induced kidney CaOx nephrocalcinosis mouse model was established and verified by polarized light microscopy (Magnification, × 100) and Pizzolato staining (Magnification, × 200) of CaOx crystal deposition in the corticomedullary junction area. PAS staining (Magnification, × 100) illustrating tubular injury. Immunohistochemical analysis of kidney HMGB1, TLR4 and NF-kB expression in a CaOx nephrocalcinosis-induced mouse model (Magnification, × 200). (c) qRT-PCR analysis was performed to detect the expression levels of HMGB1, TLR4 and NF-kB in CaOx mouse kidney samples, and these levels were compared with those in mock controls. Pearson correlation coefficient analysis of the expression levels of H19 and HMGB1 (d), TLR4 (e), and NF-kB (f). (g) qRT-PCR analysis was performed to detect the expression levels of HMGB1, TLR4 and NF-kB in HK-2 cells treated with different concentrations of COM crystals. The data are shown as the mean ± standard error (SE) of three independent experiments. (*$P < 0.05$; **$P < 0.01$, by Student's *t*-test (c) or Pearson's correlation test (d, e, f) or one-way ANOVA (g)).

Please cite this article as: H. Liu et al., H19 promote calcium oxalate nephrocalcinosis-induced renal tubular epithelial cell injury via a ceRNA pathway, EBioMedicine (2019), https://doi.org/10.1016/j.ebiom.2019.10.059

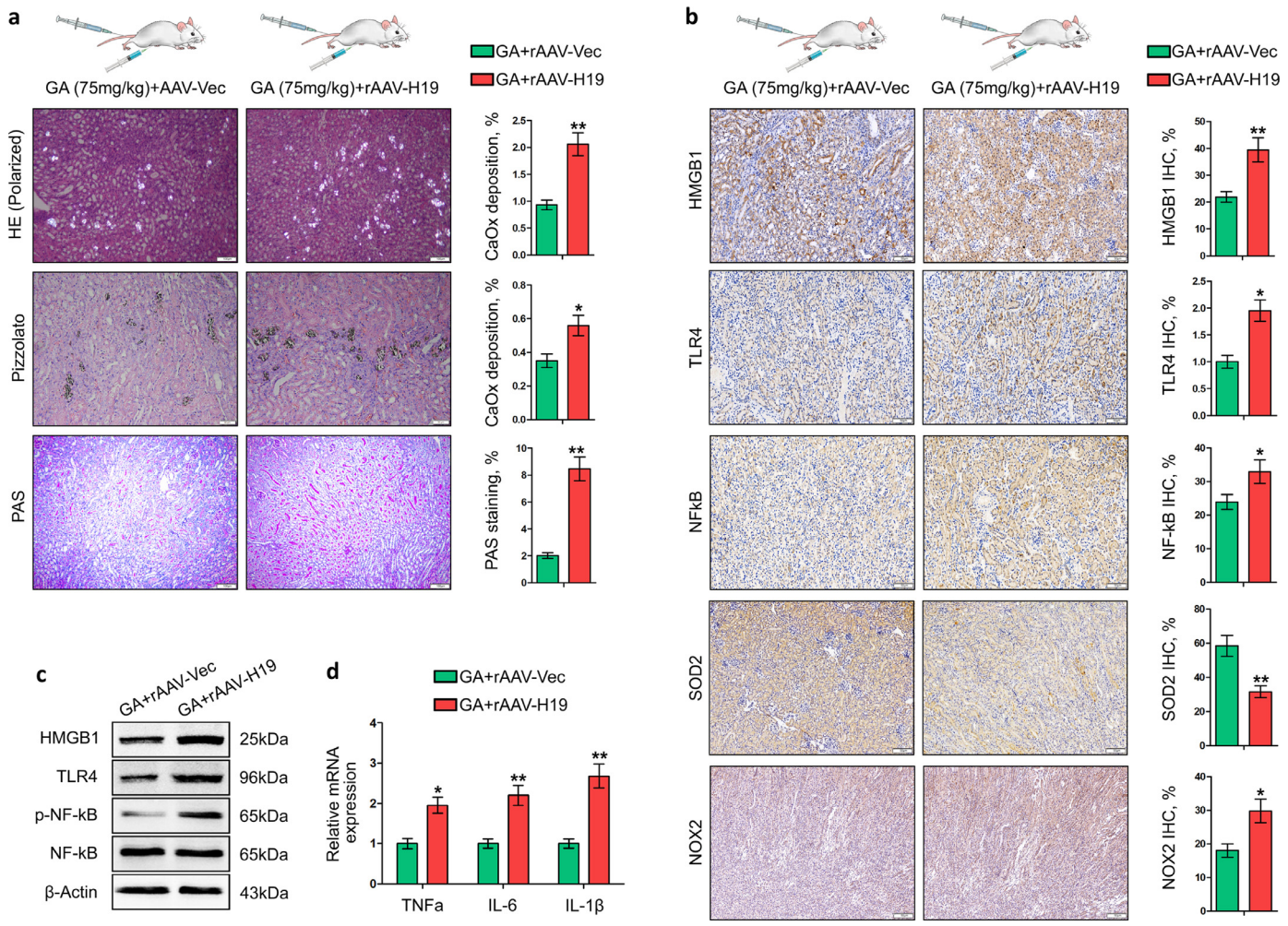

Fig. 2. H19 facilitated CaOx nephrocalcinosis-induced renal tubular epithelial cell injury *in vivo*. CaOx deposition in the corticomedullary junction area was measured by polarized light microscopy (Magnification, × 100) and Pizzolato staining (Magnification, × 200). PAS staining (Magnification, × 100) illustrating renal tubular epithelial cell injury. (b) Immunohistochemical analysis of kidney HMGB1, TLR4, NF-kB, SOD2 and NOX2 expression was performed in rAAV-H19 or rAAV-vector injected CaOx nephrocalcinosis mouse models (Magnification, × 200). (c) Western blot analysis was performed to detect HMGB1, TLR4, p-NF-kB and NF-kB protein expression in H19-treated kidney tissue. GAPDH served as an internal control. (d) qRT-PCR analysis was performed to detect the expression levels of proinflammatory cytokines in kidney tissue. The data are shown as the mean ± standard deviation (SD) of three independent experiments. (*$P < 0.05$; **$P < 0.01$, by Student's *t*-test (a, b, d)).

nephrocalcinosis-induced mouse model. Pizzolato staining and polarized light optical microphotography revealed a significant increase in CaOx crystal deposition in the kidneys (Fig. 2a). PAS staining further confirmed that H19 activation accelerated renal tubular epithelial cell injury (Fig. 2a). Additionally, increased IHC staining for HMGB1, TLR4 and NF-kB was observed in the rAAV-H19-injected mouse kidneys (Fig. 2b). We further observed strong staining for the subunit of NADPH oxidase NOX2 but weak SOD2 signals in the rAAV-H19-injected mouse kidneys (Fig. 2b). Western blot analysis showed that H19 activation by rAAV-H19 injection in CaOx nephrocalcinosis mouse kidneys significantly increased HMGB1, TLR4 and NF-kB expression ($P < 0.05$, Fig. 2c). Additionally, qRT-PCR analysis revealed that rAAV-H19 injection enhanced the release of proinflammatory cytokines, such as TNF-a, IL-6, and IL-1β, in CaOx nephrocalcinosis mouse kidneys ($P < 0.05$, Fig. 2d).

3.3. *H19 promoted COM crystal-induced renal tubular epithelial cell oxidative stress injury* in vitro

We cocultured HK-2 cells with COM crystals. Western blot and qRT-PCR analyses showed that H19 activation via lenti-H19 transfection or knockdown via H19 small interfering RNA (siRNA) transfection in HK-2 cells significantly increased or decreased, respectively, HMGB1, TLR4 and NF-kB expression ($P < 0.05$, Fig. 3a and b). To investigate the effects of H19 on CaOx-induced renal tubular cell injury, lenti-H19 transfection was performed and caused a significant increase in LDH release, cellular MDA levels, H_2O_2 concentrations and ROS generation in HK-2 cells incubated with COM crystals (Fig. 3c–g). In contrast, H19 knockdown by H19 siRNA transfection in HK-2 cells caused a significant decrease in ROS generation (Fig. 3g and h), LDH leakage, cellular MDA levels, and H_2O_2 concentration, while a significant reduction of SOD levels was observed (Fig. 3c–f). In addition, apoptosis was analysed by flow cytometry. Lenti-H19 and H19 siRNA transfection significantly promoted or attenuated, respectively, COM crystal-induced necrosis (Fig. 3i). Therefore, the activation of H19 could induce ROS burst and renal tubular cell injury and further promote CaOx crystal deposition in the kidneys.

3.4. *H19 directly bound to the 3′-UTR of miR-216b to suppress its expression*

The interaction between lncRNAs and microRNAs is a major mechanism by which lncRNAs exert their effects. To further investigate the mechanism by which H19 regulates the progression of CaOx nephrocalcinosis, we focused on miR-216b. Starbase 2.0 predicted that miR-216b is a potential target of H19 (Fig. 4a). Additionally, qRT-PCR assays showed that the expression of miR-216b was remarkably decreased in

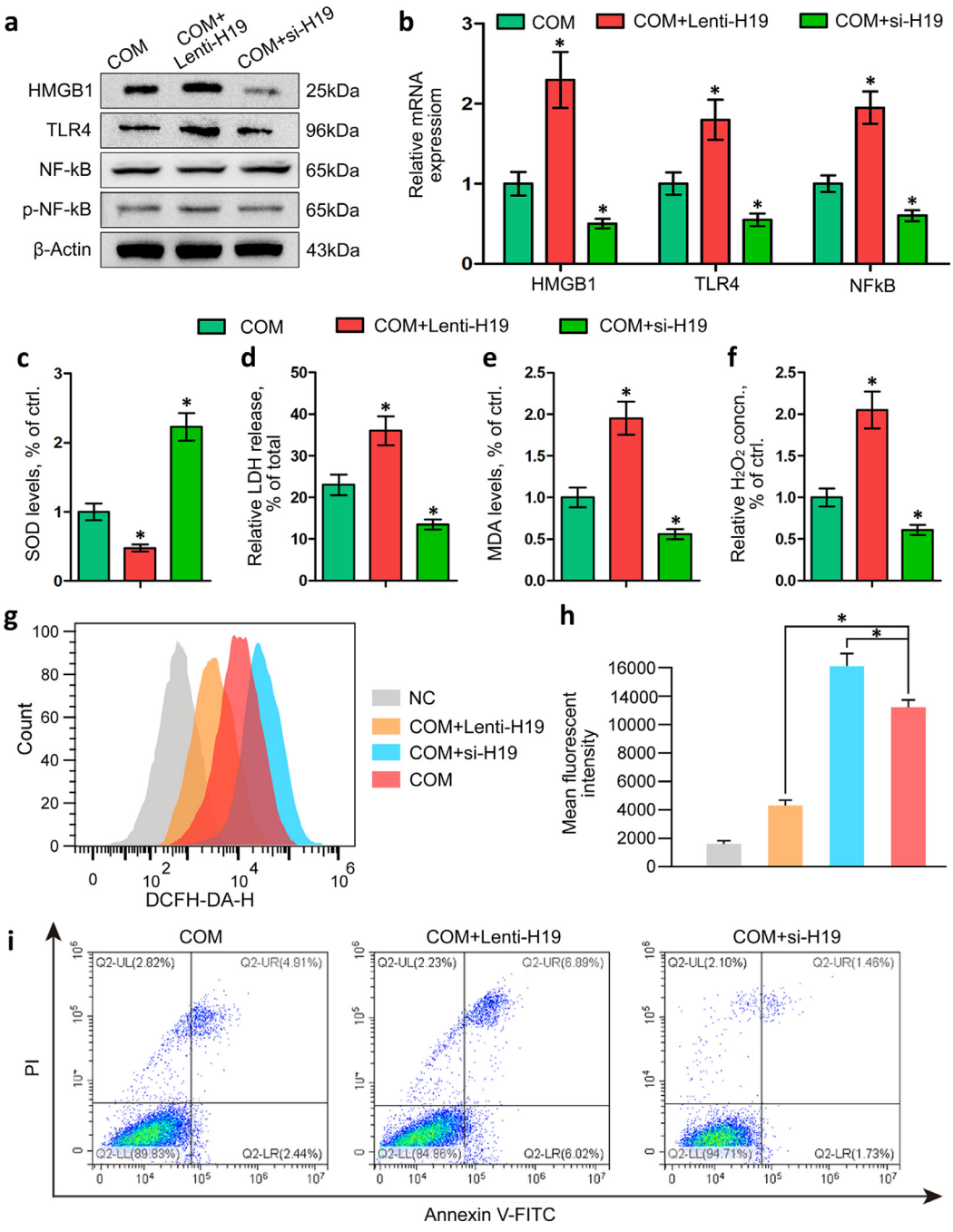

Fig. 3. H19 promoted COM crystal-induced renal tubular epithelial cell oxidative stress injury *in vitro*. Western blot (a) and qRT-PCR (b) analyses of HMGB1, TLR4, NF-kB and p-NF-kB expression in HK-2 cells. β-Actin was used for normalization. SOD level (c), LDH release (d), MDA level (e), and H_2O_2 concentration (f) were determined in HK-2 cells incubated with COM crystals following lenti-H19 and si-H19 treatment. (g) Cellular ROS production in HK-2 cells was measured by flow cytometry. (h) Histograms showing the mean fluorescence intensity of DCFH. (i) The apoptosis effect was investigated by flow cytometric analysis of HK-2 cells stained with Annexin V-FITC and propidium iodide. ($^{*}P < 0.05$; $^{**}P < 0.01$, by one-way ANOVA (b-f, h, i)).

CaOx nephrocalcinosis mouse kidney tissues (Fig. 4b) and negatively correlated with H19 expression (Fig. 4c). Decreased miR-216b expression was observed after H19 siRNA transfection (Fig. 4d). Subsequently, miR-216b was up- and downregulated with miR-216b mimics and inhibitor, respectively. The qRT-PCR assays confirmed the suppression of H19 expression following miR-216b upregulation, while increased H19 expression was noted following miR-216b downregulation (Fig. 4e). To investigate the interaction between H19 and miR-216b, a wild-type (WT) H19 3′-UTR luciferase reporter vector and a mutant H19 3′-UTR luciferase reporter vector (mutated on the miR-216b binding site of the H19 3′-UTR) were constructed. When cotransfected with the miR-216b mimics, the luciferase activity of the WT H19 vector was significantly suppressed, while no significant change was observed with the mutant H19 vector (Fig. 4f); when cotransfected with the miR-216b inhibitor, the luciferase activity of the WT H19 vector was promoted, and no significant change was observed with the mutant H19 vector (Fig. 4g). These results indicate that H19 directly bound the 3′-UTR of miR-216b to suppress its expression.

3.5. *miR-216b inhibited HMGB1 expression by directly binding its 3′-UTR*

Since we found that H19 is positively correlated with HMGB1 expression but inversely correlated with miR-216b expression, we aimed to further investigate the exact role of the H19 and miR-216b

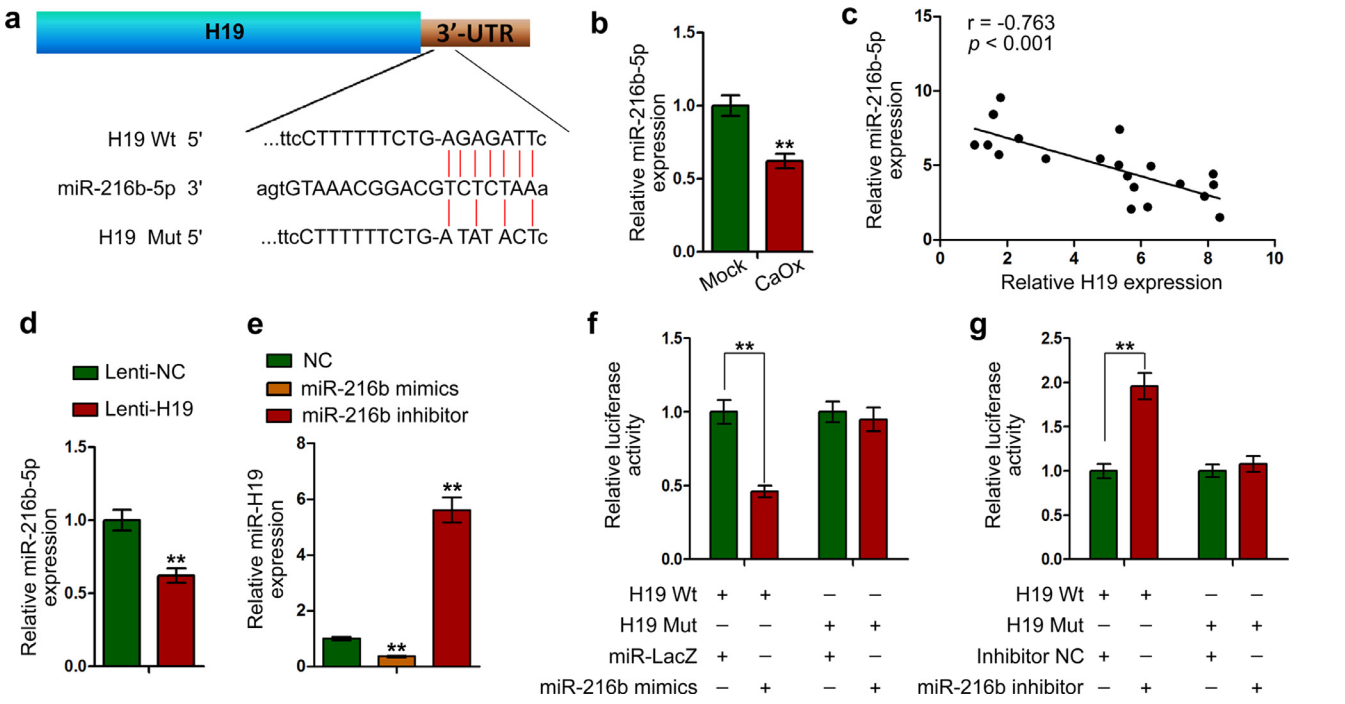

Fig. 4. H19 interacted with miR-216b by directly binding its 3′-UTR. Schematic diagram of the mutant and WT seed sequences of miR-216b targeting the 3′-UTR of H19. (b) qRT-PCR analysis was performed to detect the expression level of miR-216b in CaOx-induced mouse kidney samples, and this expression was compared with that in the mock control. U6 was used as a miRNA control. (c) Pearson correlation coefficient analysis of the expression levels of H19 and miR-216b. (d) miR-216b expression was inhibited by lenti-H19 transfection. (e) H19 expression was detected using qRT-PCR in HK-2 cells transfected with the miR-216b mimics and inhibitor. Luciferase reporters harbouring putative target sites in the WT and mutant 3′-UTR of H19 were cotransfected with 100 nM miR-216b mimics (f) or miR-216b inhibitor (g) in HK-2 cells. The data are shown as the mean ± SD of three independent experiments. (*$P < 0.05$; **$P < 0.01$, by Student's *t*-test (b) or Pearson's correlation test (c) or one-way ANOVA (d-g)).

regulatory factor HMGB1. The bioinformatics analysis showed that HMGB1 contains conserved putative miR-216b target sites in its 3′-UTR. We first constructed luciferase reporter plasmids containing either the WT or mutated miR-216b target sequences in the 3′-UTR of HMGB1 (Fig. 5a and b). When cotransfected with the miR-216b mimics, the luciferase activity of the WT-HMGB1 vector was notably suppressed, while no significant change was observed when cotransfected with the miR-216b inhibitor compared with the control group (Fig. 5c). In addition, miR-216b and HMGB1 expression levels were negatively correlated in glyoxylate-induced CaOx nephrocalcinosis mouse kidney samples (Fig. 5d). Western blot and qRT-PCR assays demonstrated that compared with the control group, the mRNA and protein expression levels of HMGB1, TLR4 and NF-kB were significantly elevated by the miR-216b inhibitor but repressed by the miR-216b mimics in HK-2 cells (Fig. 5e-i). Altogether, these results reveal that miR-216b inhibits HMGB1 expression by directly binding to its 3′-UTR.

3.6. *miR-216b suppressed COM crystal-induced renal tubular epithelial cell oxidative stress injury* in vitro

To investigate the effects of miR-216b on CaOx-induced renal tubular cell injury, miR-216b mimics and inhibitor were transfected into HK-2 cells and incubated with COM crystals. miR-216b activation significantly reduced LDH release, cellular MDA levels, and H_2O_2 concentrations but increased cellular SOD levels (Fig. 6a–d). In contrast, miR-216b knockdown in HK-2 cells significantly induced LDH leakage, cellular MDA levels, and H_2O_2 concentrations but decreased cellular SOD levels (Fig. 6a–d). A flow cytometric analysis of ROS was carried out, and ROS generation in cells transfected with the miR-216b mimics was significantly lower than that in the control cells (Fig. 6e and f). In addition, apoptosis was analysed by flow cytometry. Transfection with the miR-216b mimic or inhibitor significantly decreased or increased, respectively, COM crystal-induced necrosis (Fig. 6g). Therefore, the activation of miR-216b could attenuate the ROS burst, protect against renal tubular cell injury, and further decrease CaOx crystal deposition in the kidneys.

3.7. *miR-216b reversed the effect of H19 on CaOx nephrocalcinosis-induced renal tubular epithelial cell injury* in vivo

To explore the effects of H19-sponged miR-216b downregulation on CaOx crystal formation in the kidney and CaOx nephrocalcinosis-induced renal tubular cell injury, rAAV-H19, the miR-216b agonist, or both were injected through the tail vein in the glyoxylate-induced CaOx nephrocalcinosis mouse model *in vivo*. The Pizzolato staining and polarized light optical microphotography revealed that the miR-216b agonist significantly decreased CaOx crystal deposition in the kidneys (Fig. 7a). The PAS staining further confirmed that miR-216b activation protected against renal tubular epithelial cell injury (Fig. 7a). Additionally, decreased IHC staining of HMGB1, TLR4, NF-kB and NOX2 but strong SOD2 signals were observed in the kidney of miR-216b agonist-treated mice (Fig. 7b). Compared to rAAV-H19 treatment, miR-216b agonist treatment led to significant decreases in CaOx crystal deposition in the kidney, PAS staining and HMGB1, TLR4 and NF-kB expression, suggesting that miR-216b activation abrogates the effect of H19 on promoting CaOx nephrocalcinosis-induced renal tubular epithelial cell injury.

3.8. *Anti-HMGB1 reversed the effect of H19 activation on CaOx nephrocalcinosis-induced renal tubular epithelial cell injury* in vivo

To explore the effects of HMGB1 on CaOx crystal formation in the kidney and CaOx nephrocalcinosis-induced renal tubular cell injury, a neutralizing antibody of HMGB1 was used to reduce its expression CaOx nephrocalcinosis mouse model. And then, rAAV-H19, anti-HMGB1, or both were injected through the tail vein in the glyoxylate-induced CaOx nephrocalcinosis mouse model in *vivo*. The polarized light optical microphotography and Pizzolato staining found that anti-HMGB1 significantly

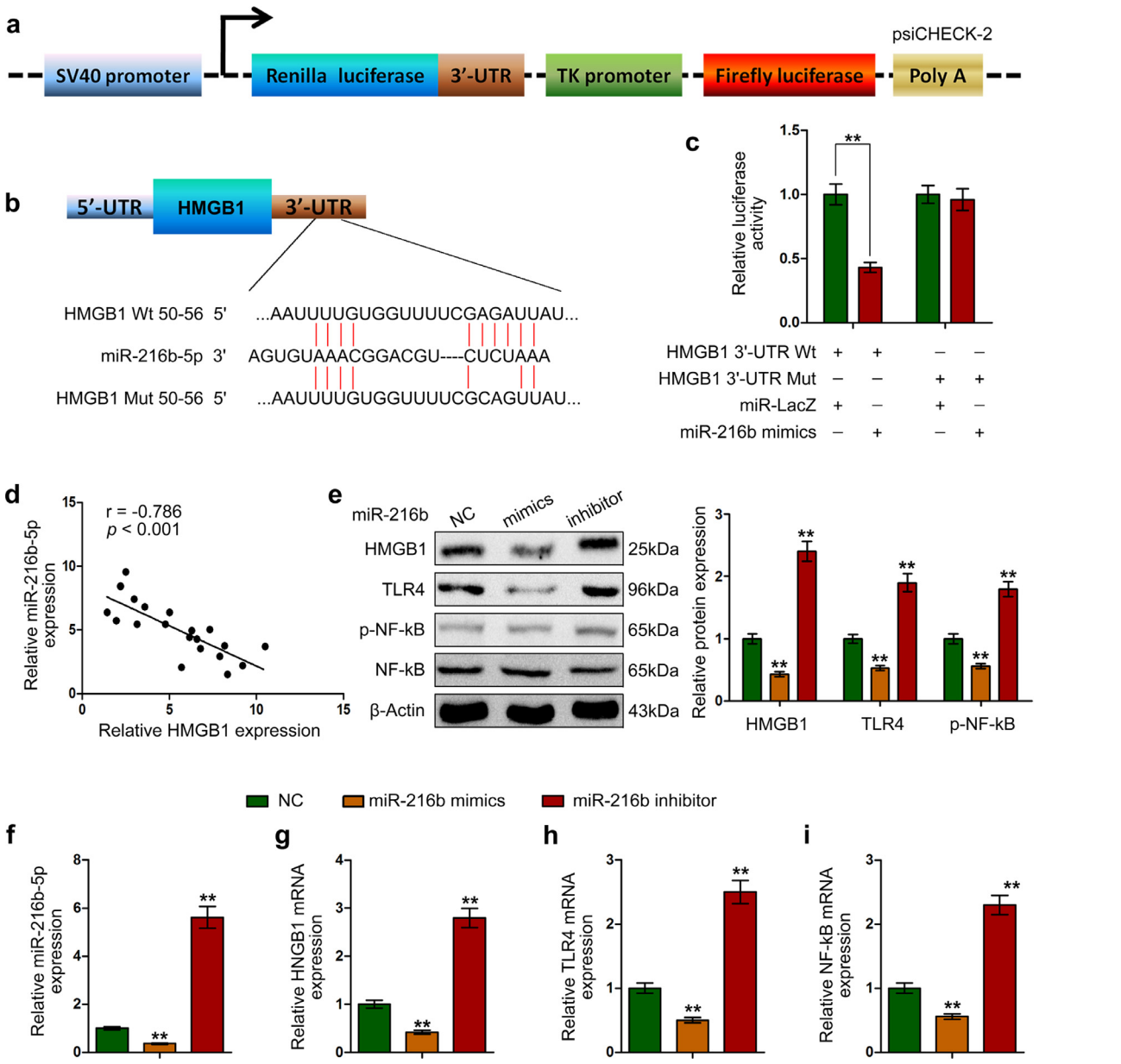

Fig. 5. miR-216b inhibited HMGB1 expression by directly binding to its 3′-UTR. Schematic diagram of our constructed luciferase reporter plasmid psiCHECK-2 containing the 3′-UTR of HMGB1. (b) Mutant and WT seed sequences of miR-216b targeting the 3′-UTR of HMGB1. (c) Luciferase reporters harbouring putative target sites in the WT and mutant 3′-UTRs of HMGB1 were cotransfected with 100 nM of the indicated small RNA molecules in HK-2 cells. (d) Pearson correlation coefficient analysis of the expression levels of H19 and miR-216b. (e) Western blot analysis was performed to detect the expression of HMGB1, TLR4, NF-kB and p-NF-kB in HK-2 cells transfected with the miR-216b mimics or inhibitor. Actin-β served as an internal control. (f) miR-216b mimics and inhibitor were used to establish miR-216b overexpression and inhibition, respectively, in HK-2 cells. The expression of HMGB1 (g), TLR4 (h), and NF-kB (i) was detected using qRT-PCR in HK-2 cells transfected with miR-216b mimics or inhibitor. The data are shown as the mean ± SD of three independent experiments. ($^{*}P < 0.05$; $^{**}P < 0.01$, by one-way ANOVA (c, e-i) or Pearson's correlation test (d)).

decreased CaOx crystal deposition in the kidneys (Supplementary Fig. S2a). The PAS staining further demonstrated that HMGB1 inhibition protected against renal tubular epithelial cell injury (Supplementary Fig. S2a). Additionally, decreased IHC staining of HMGB1, TLR4, NF-kB and NOX2 but strong SOD2 signals were observed in the kidney in anti-HMGB1-treated mice (Supplementary Fig. S2b). The inhibition of HMGB1 reversed the effect of H19 on promoting CaOx nephrocalcinosis-induced renal tubular epithelial cell injury.

3.9. *miR-216b reversed the effect of H19 on COM crystal-induced renal tubular epithelial cell oxidative stress injury* in vitro

To further investigate the effects of H19-sponged miR-216b on COM crystal-induced renal tubular epithelial cell oxidative stress injury, lenti-H19, miR-216b mimics or both were cotransfected into HK-2 cells and incubated with COM crystals. Western blot and qRT-PCR analyses showed that HMGB1, TLR4 and NF-kB expression was upregulated following treatment with lenti-H19 in HK-2 cells, while their expression was downregulated following treatment with the miR-216b mimics (Fig. 8a and b). These effects were abrogated after cotransfection of lenti-H19 and miR-216b mimics (Fig. 8a and b). Additionally, lenti-H19 treatment significantly increased ROS generation, LDH release, cellular MDA levels, and H_2O_2 concentration in HK-2 cells incubated with COM crystals (Fig. 8c–h). In contrast, miR-216b mimics treatment in HK-2 cells led to significantly decreased ROS generation, reduced LDH leakage, and lower MDA and H_2O_2 levels in cells (Fig. 8c–h). Transfection with the miR-216b mimics significantly decreased COM crystal-induced necrosis compared with

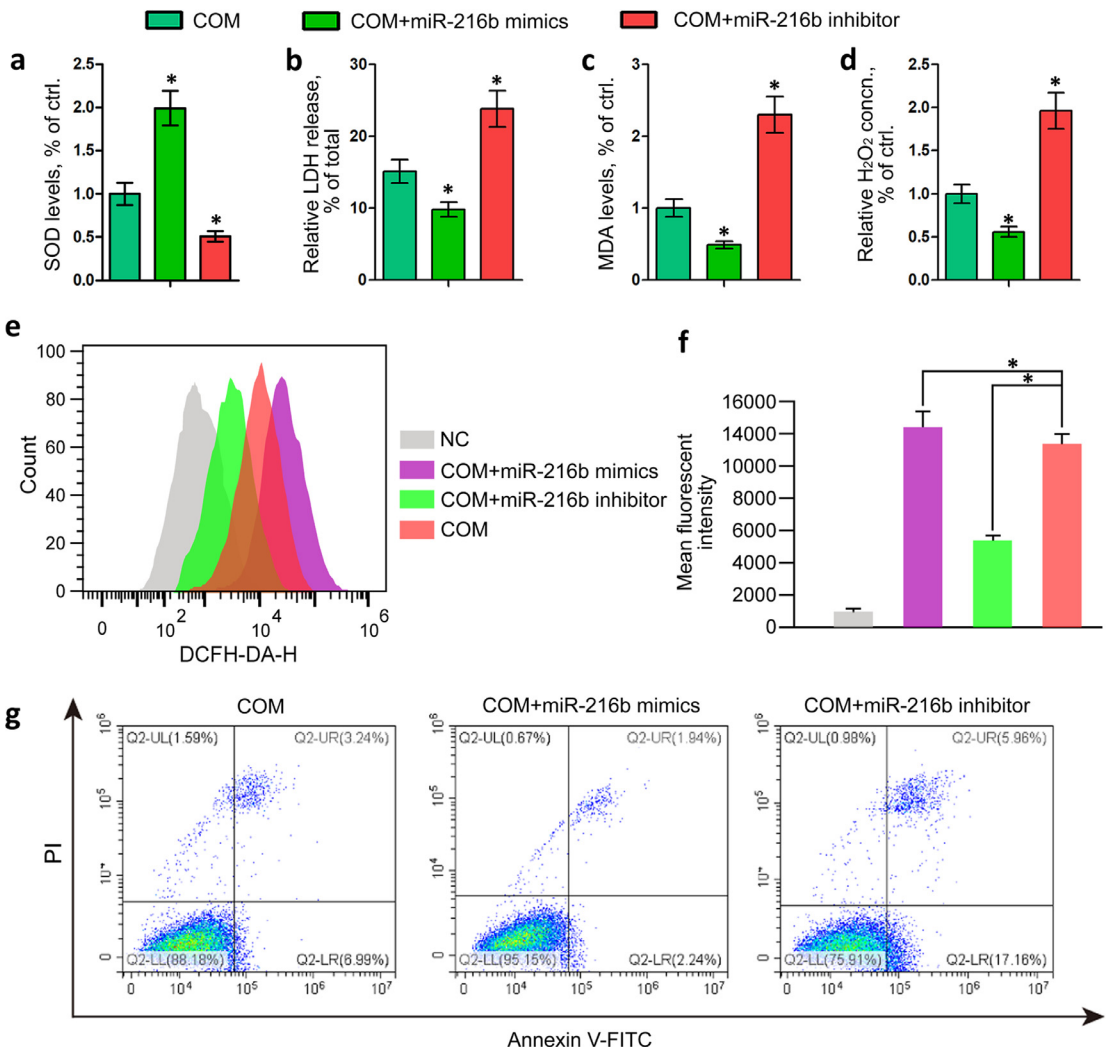

Fig. 6. miR-216b suppressed COM crystal-induced renal tubular epithelial cell oxidative stress injury *in vitro*. (a) SOD level, (b) LDH release, (c) MDA level, and (d) H_2O_2 concentration were determined in HK-2 cells incubated with COM crystals following miR-216b mimics or inhibitor treatment. (e-f) Cellular ROS production in HK-2 cells was measured by flow cytometry. Histograms showing the mean fluorescence intensity of DCFH. (g) Apoptosis was analysed by flow cytometry in HK-2 cells transfected with miR-216b mimics or inhibitor. Histograms showing the mean fluorescence intensity. The data are shown as the mean ± SD of three independent experiments. (*$P < 0.05$; **$P < 0.01$, by one-way ANOVA (a-d, f, g)).

lenti-H19 treatment in HK-2 cells (Fig. 8i), indicating that miR-216b could reverse the effect of H19 on COM crystal-induced renal tubular epithelial cell oxidative stress injury. Therefore, the activation of miR-216b can attenuate the ROS burst, protect against renal tubular cell injury, and further decrease CaOx crystal deposition in the kidneys (Fig. 9).

4. Discussion

Experimental and clinical study results have shown that kidney tubular epithelial cell exposure to CaOx crystals can generate excess ROS, causing inflammation and inducing injury [17,18]. HMGB1-mediated intrarenal inflammation contributes to acute and chronic oxalosis in mice and causes the proinflammatory factors TLR4 and NF-kB to induce tubular epithelial necroptosis and promote CaOx deposition [19]. Similar to previous studies [8], we found that the HMGB1/TLR4/NF-kB pathway was increased and involved in CaOx nephrocalcinosis pathogenesis.

Recent studies have found that lncRNAs are deregulated in organ injury and regulate inflammatory cytokine production [20, 21]. Here, we first investigated the regulatory role of lncRNAs in kidney stone pathogenesis. We report that H19 expression was significantly increased and positively correlated with HMGB1, TLR4 and NF-κB expression in a glyoxylate-induced CaOx nephrocalcinosis mouse model. Consistent with our results, H19 has been recognized as an inflammatory regulator that triggers the immune response and induces tissue injury [10–12]. In addition, a recent study reported that autophagy was an important regulator in the formation and progression of kidney stone disease, and the inhibition of autophagy could decrease kidney injury and crystal deposition in an ethylene glycol-induced rat model of nephrolithiasis [22]. H19 was also reported to be involved in the regulation of autophagy. Zhang L et al. found that in placentas from a foetal growth restriction model, the downregulation of H19 could suppress cell proliferation and invasion and activate autophagy by regulating the miR-18a-5p/IRF2 axis [23]. Wang J et al. reported that H19 could inhibit autophagy to induce cerebral ischaemia and reperfusion (I/R) injury [12]. In our study, we identified the promotive role of H19 in calcium oxalate-induced renal tubular epithelial cell injury and crystal deposition in a glyoxylate-induced nephrolithiasis mouse model. Considering these previous studies, autophagy regulation by H19 might be involved in the pathophysiological process of kidney stone disease.

The interactions between lncRNAs and miRNAs play an important role in regulating the expression of related genes at the transcriptional and posttranscriptional levels. It has been reported that

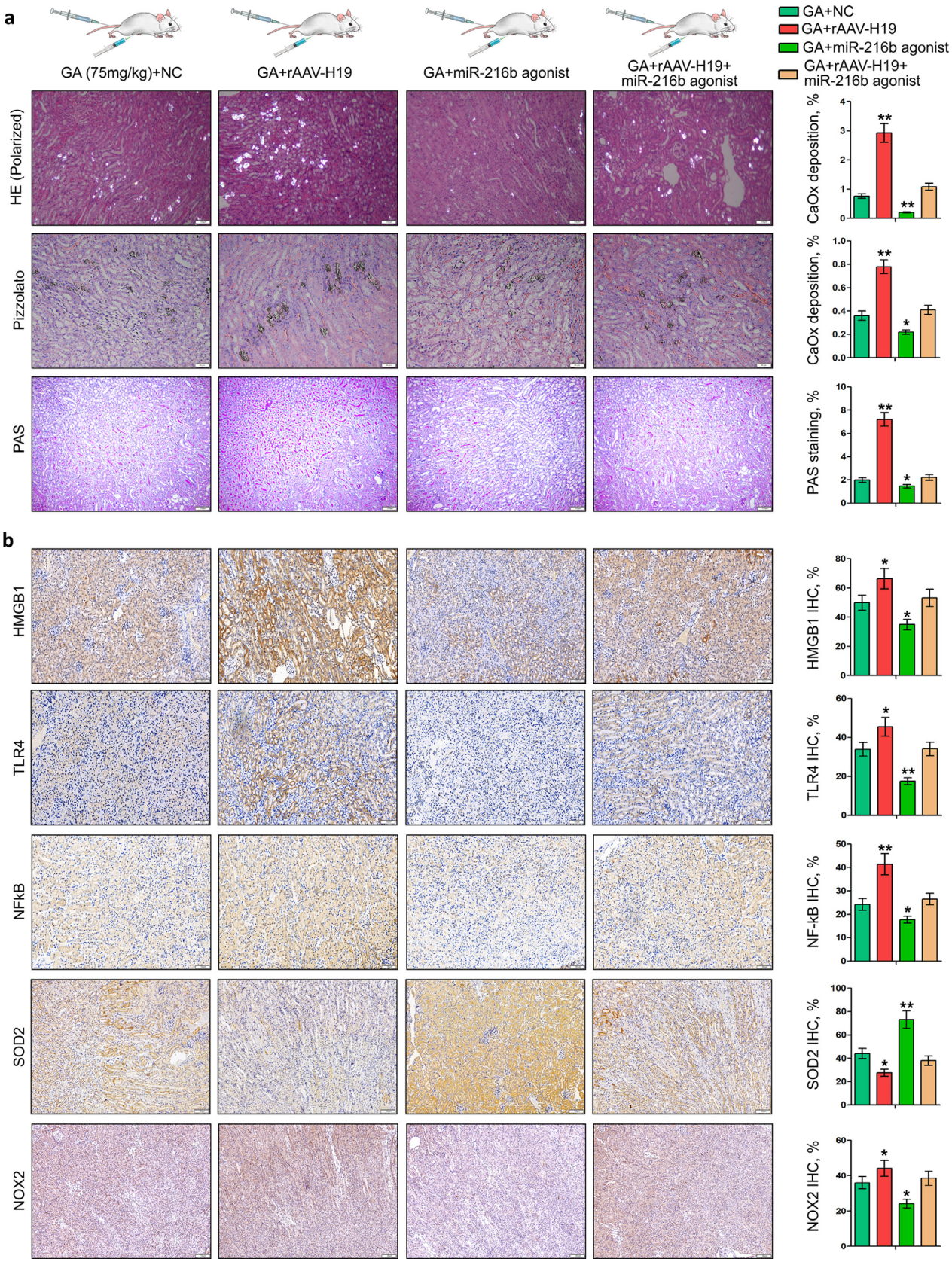

Fig. 7. miR-216b reversed the effect of H19 on CaOx nephrocalcinosis-induced renal tubular epithelial cell injury *in vivo*. (a) CaOx deposition in the corticomedullary junction area was measured by polarized light microscopy (Magnification, × 100) and Pizzolato staining (Magnification, × 200). PAS staining (Magnification, × 100) illustrating renal tubular epithelial cell injury. (b) Immunohistochemical analysis of kidney HMGB1, TLR4, NF-kB, SOD2 and NOX2 expression was performed in rAAV-H19-, miR-216b agonist-, or combination-treated CaOx nephrocalcinosis mouse models (magnification in all panels is 200 ×). Quantifications were performed using ImageJ. The data are shown as the mean ± SD of three independent experiments. (*$P < 0.05$; **$P < 0.01$, by one-way ANOVA (a, b)).

Please cite this article as: H. Liu et al., H19 promote calcium oxalate nephrocalcinosis-induced renal tubular epithelial cell injury via a ceRNA pathway, EBioMedicine (2019), https://doi.org/10.1016/j.ebiom.2019.10.059

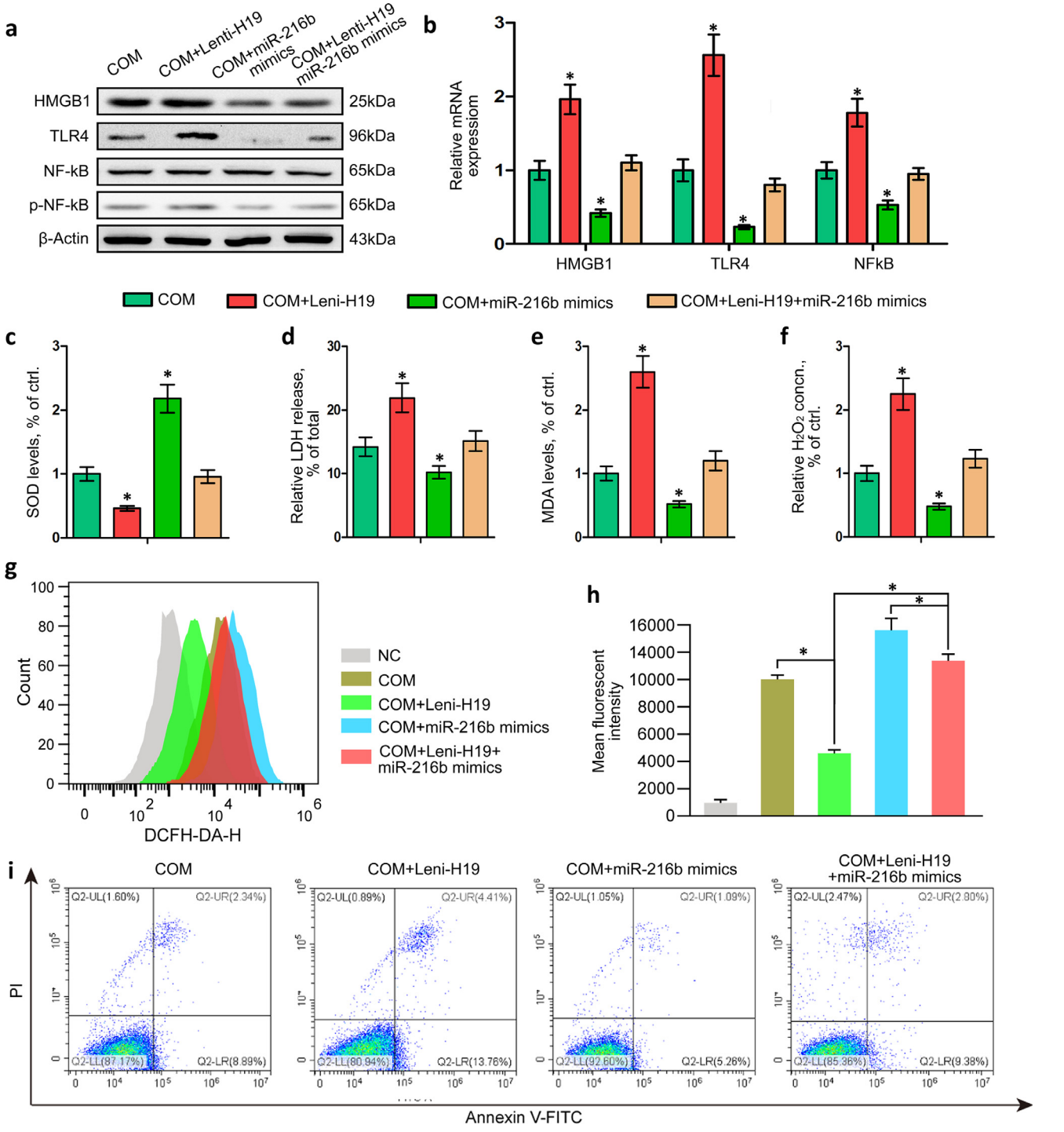

Fig. 8. miR-216b reversed the effect of H19 on COM crystal-induced renal tubular epithelial cell oxidative stress injury *in vitro*. Western blot (a) and qRT-PCR (b) analyses of HMGB1, TLR4 and NF-kB expression in HK-2 cells following transfection with lenti-H19, miR-216b mimics, or their combination. β-Actin was used for normalization. ROS generation (c), LDH release (d), cellular malondialdehyde (MDA) levels (e), and H_2O_2 concentrations (f) were determined in HK-2 cells incubated with COM crystals following treatment with lenti-H19, miR-216b mimics or their combination. (G-H) Flow cytometric analysis of cellular ROS generation was carried out in HK-2 cells. Histograms showing the mean fluorescence intensity of DCFH. (g) The apoptosis effect was investigated by flow cytometric analysis of HK-2 cells stained with Annexin V-FITC and propidium iodide. The data are shown as the mean ± SD of three independent experiments. (*$P < 0.05$; **$P < 0.01$, by one-way ANOVA (b–i)).

lncRNAs act as endogenous miRNA sponges to target miRNAs and are involved in a competitive endogenous RNA (ceRNA) mechanism to negatively modulate miRNA expression [24]. Wan Pet al. found that the lncRNA H19/miR-21/PDCD4 ceRNA pathway could regulate retinal ischaemia/reperfusion-induced sterile inflammation [25]. Lu YF et al. reported that H19 targets miR-29b-3p by acting as a miRNA sponge and activates TGF-β1 signalling to promote tendon healing [26]. Wang SH et al. found that H19 regulates FOXM1 expression by competitively binding miR-342 in gallbladder cancer [27]. H19 has also been found to competitively bind to miR-17 and regulate YES1 expression in thyroid carcinogenesis [28].

To identify the potential target miRNAs of H19 in the regulation of CaOx nephrocalcinosis pathogenesis, a bioinformatics analysis was performed, and miR-216b was identified as a target of H19. Our

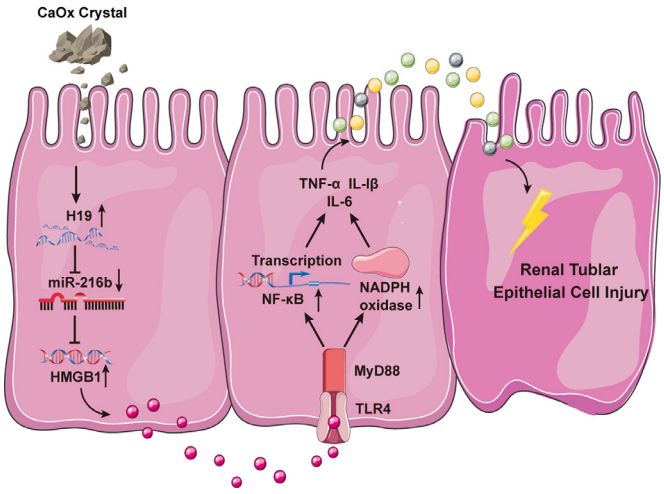

Fig. 9. Schematic model. LncRNA H19 sponges miR-216b-3p to promote calcium oxalate nephrocalcinosis-induced renal tubular epithelial cell injury via HMGB1/TLR4/NF-κB pathway activation.

results indicate that H19 significantly suppresses miR-216b expression and that knocking down H19 led to miR-216b overexpression. Luciferase reporter assays verified that H19 downregulated miR-216b expression by directly binding to its 3′-UTR, which participates in a regulatory network of ceRNAs. miR-216b has been well characterized as an inflammatory regulator and a tumour suppressor gene. Several previous studies have demonstrated that miR-216b is associated with the progression of inflammatory disease and suppresses tissue injury [29,30]. He J. et al. reported that miR-216b directly targets Smad3 expression and inhibits IL-1β-induced chondrocyte injury [31]. Plasma miR-216b could be used as a biomarker to identify kidney injury [30]. Notably, our results indicate that miR-216b expression was markedly downregulated in the glyoxylate-induced CaOx nephrocalcinosis mouse kidneys and inversely correlated with H19 and HMGB1 expression.

However, the role of miR-216b in CaOx nephrocalcinosis disease pathogenesis is still unknown. Moreover, bioinformatics analysis and luciferase reporter assays indicate that miR-216b directly targets HMGB1. miR-216b overexpression resulted in decreased HMGB1 expression and suppressed the TLR4/NF-kB signalling pathway. Our present results also revealed that miR-216b overexpression partially blocked the inhibitory effect of H19 knockdown on HMGB1 expression and tubular epithelial cell injury and remarkably inhibited kidney CaOx crystal deposition *in vitro*. These data indicate that miR-216b might be a critical player in intrarenal inflammation and kidney tubular cell injury. Several inflammatory genes have been found to be direct targets of miR-216b. He J. et al. found that miR-216b inhibits IL-1β-induced chondrocyte injury by targeting Smad3 expression [29]. Xu et al. previously demonstrated that miR-216b regulates c-Jun-mediated GADD153/CHOP-dependent apoptosis [31]. Moreover, as an inflammatory biomarker of acute pancreatitis and pancreatic injury, circulating miR-216b has been evaluated in both murine models and patients [32–34].

Recent findings indicated that NLRP3 inflammasome activation was considered to be a critical factor in calcium oxalate crystal induce renal inflammation by promoting proinflammatory cytokine section and ROS production [16,35]. H19 was also found to regulate neuroinflammation by balancing the activation of NLRP3/NLRP6 inflammasomes [25]. Moreover, a study reported by Chi W et al. showed that HMGB1 could significantly induce increased NLRP3 levels and IL-1β production, which contribute to the development of acute glaucoma [15]. Therefore, increased H19 and HMGB1 expression might induce NLRP3 inflammasome activation to contribute to CaOx nephrocalcinosis-induced kidney injury.

In this work, we described the facilitatory role of H19 in CaOx nephrocalcinosis-induced renal tubular epithelial cell injury and glyoxylate-induced kidney CaOx crystal deposition. We also revealed the mechanism by which the H19 and miR-216b interaction exerts its effect by regulating the HMGB1/TLR4/NF-κB pathway. Our study provides new mechanistic insight into the regulatory role of lncRNAs in CaOx nephrocalcinosis disease and may aid in the development of novel therapeutic strategies targeting lncRNAs. However, limitation of this study was not considered in human, and further studies should be conducted in clinical CaOx kidney stone formers to support this evidence.

Funding sources

This work was supported by the National Nature Science Foundation of China(8196030190, 8190033175, 81370805, 81470935, 81900645, 81500534, and 81602236). The funder had no role in the study design, data collection, data analysis, interpretation and writing of the report.

Authors' contributions

This work was carried out in collaboration among all authors. Kun Tang, Haoran Liu contributed to the conception and design of the study. Kun Tang participated in the drafting of the article. Haoran Liu, Tao Ye, Xiaoqi Yang and Kehua Jiang carried out the experiments. Kun Tang contributed to all figures and tables. Jianhe Liu, Ejun Pneg, Zhiqiang Chen, Fa Sun and Zhangqun Ye revised the manuscript. Honglu Lu, Ding Xia contributed to data collection and analysis. All authors have read and approved the final manuscript.

Declaration of Competing Interest

The authors have nothing to disclose.

CRediT authorship contribution statement

Haoran Liu: Conceptualization, Funding acquisition, Project administration, Resources, Software, Writing - original draft. **Tao Ye:** Investigation, Methodology, Funding acquisition, Project administration, Resources, Software. **Xiaoqi Yang:** Investigation, Methodology. **Jianhe Liu:** Supervision, Visualization, Visualization. **Hongyan Lu:** Data curation, Formal analysis. **Ding Xia:** Data curation, Formal analysis. **Ejun Peng:** Supervision, Visualization, Visualization. **Zhiqiang Chen:** Supervision, Visualization, Visualization. **Fa Sun:** Supervision, Visualization, Visualization. **Kun Tang:** Conceptualization, Funding acquisition, Project administration, Resources, Software, Writing - original draft. **Zhangqun Ye:** Funding acquisition, Supervision, Visualization, Visualization.

Acknowledgements

We thank all other researchers in our laboratory.

Supplementary materials

Supplementary material associated with this article can be found in the online version at doi:10.1016/j.ebiom.2019.10.059.

References

[1] Khan SR, Pearle MS, Robertson WG, et al. Kidney stones. Nat Rev Dis Primers 2016;2:16008.
[2] Zeng G, Mai Z, Xia S, et al. Prevalence of kidney stones in China: an ultrasonography based cross-sectional study. BJU Int 2017;120(1):109–16.
[3] Mulay SR, Eberhard JN, Desai J, et al. Hyperoxaluria requires tnf receptors to initiate crystal adhesion and kidney stone disease. J Am Soc Nephrol 2017;28(3):761–8.

[4] Ruan Y, Wang L, Zhao Y, et al. Carbon monoxide potently prevents ischemia-induced high-mobility group box 1 translocation and release and protects against lethal renal ischemia-reperfusion injury. Kidney Int 2014;86(3):525–37.
[5] Chen X, Wu S, Chen C, et al. Omega-3 polyunsaturated fatty acid supplementation attenuates microglial-induced inflammation by inhibiting the HMGB1/TLR4/NF-kappaB pathway following experimental traumatic brain injury. J Neuroinflammation 2017;14(1):143.
[6] Lundback P, Lea JD, Sowinska A, et al. A novel high mobility group box 1 neutralizing chimeric antibody attenuates drug-induced liver injury and postinjury inflammation in mice. Hepatology 2016;64(5):1699–710.
[7] Jiang Z, Zhou Q, Gu C, et al. Depletion of circulating monocytes suppresses IL-17 and HMGB1 expression in mice with LPS-induced acute lung injury. Am J Physiol Lung Cell Mol Physiol 2017;312(2):L231–L42.
[8] Wang Y, Sun C, Li C, et al. Urinary MCP-1HMGB1 increased in calcium nephrolithiasis patients and the influence of hypercalciuria on the production of the two cytokines. Urolithiasis 2017;45(2):159–75.
[9] Keniry A, Oxley D, Monnier P, et al. The H19 lincRNA is a developmental reservoir of miR-675 that suppresses growth and igf1r. Nat Cell Biol 2012;14(7):659–65.
[10] Wang J, Zhao H, Fan Z, et al. Long noncoding rna H19 promotes neuroinflammation in ischemic stroke by driving histone deacetylase 1-Dependent M1 microglial polarization. Stroke 2017;48(8):2211–21.
[11] Song Y, Liu C, Liu X, et al. H19 promotes cholestatic liver fibrosis by preventing ZEB1-mediated inhibition of epithelial cell adhesion molecule. Hepatology 2017;66(4):1183–96.
[12] Wang J, Cao B, Han D, et al. Long non-coding RNA H19 induces cerebral ischemia reperfusion injury via activation of autophagy. Aging Dis 2017;8(1):71–84.
[13] Taguchi K, Hamamoto S, Okada A, et al. Genome-Wide gene expression profiling of randall's plaques in calcium oxalate stone formers. J Am Soc Nephrol 2017;28(1):333–47.
[14] Takamori S, Shoji F, Okamoto T, et al. HMGB1 blockade significantly improves luminal fibrous obliteration in a murine model of bronchiolitis obliterans syndrome. Transpl Immunol 2019;53:13–20.
[15] Chi W, Chen H, Li F, et al. HMGB1 promotes the activation of NLRP3 and caspase-8 inflammasomes via NF-kappaB pathway in acute glaucoma. J Neuroinflammation 2015;12:137.
[16] Mulay SR, Kulkarni OP, Rupanagudi KV, et al. Calcium oxalate crystals induce renal inflammation by NLRP3-mediated IL-1beta secretion. J Clin Invest 2013;123(1):236–46.
[17] Khan SR. Reactive oxygen species, inflammation and calcium oxalate nephrolithiasis. Transl Androl Urol 2014;3(3):256–76.
[18] Chen Z, Yuan P, Sun X, et al. Pioglitazone decreased renal calcium oxalate crystal formation by suppressing M1 macrophage polarization via the PPAR-gamma-miR-23 axis. Am J Physiol Renal Physiol 2019;317(1):F137–F51.
[19] Mulay SR, Desai J, Kumar SV, et al. Cytotoxicity of crystals involves RIPK3-MLKL-mediated necroptosis. Nat Commun 2016;7:10274.
[20] Li X, Liu R, Yang J, et al. The role of long noncoding RNA H19 in gender disparity of cholestatic liver injury in multidrug resistance 2 gene knockout mice. Hepatology 2017;66(3):869–84.
[21] Zhang L, Yang Z, Trottier J, et al. Long noncoding RNA MEG3 induces cholestatic liver injury by interaction with PTBP1 to facilitate shp mRNA decay. Hepatology 2017;65(2):604–15.
[22] Liu Y, Liu Q, Wang X, et al. Inhibition of autophagy attenuated ethylene glycol induced crystals deposition and renal injury in a rat model of nephrolithiasis. Kidney Blood Press Res 2018;43(1):246–55.
[23] Zhang L, Deng X, Shi X, et al. Silencing H19 regulated proliferation, invasion, and autophagy in the placenta by targeting miR-18a-5p. J Cell Biochem 2019;120(6):9006–15.
[24] Tay Y, Rinn J, Pandolfi PP. The multilayered complexity of ceRNA crosstalk and competition. Nature 2014;505(7483):344–52.
[25] Wan P, Su W, Zhang Y, et al. LncRNA H19 initiates microglial pyroptosis and neuronal death in retinal ischemia/reperfusion injury. Cell Death Differ 2019.
[26] Lu YF, Liu Y, Fu WM, et al. Long noncoding RNA H19 accelerates tenogenic differentiation and promotes tendon healing through targeting miR-29b-3p and activating TGF-beta1 signaling. FASEB J 2017;31(3):954–64.
[27] Wang SH, Ma F, Tang ZH, et al. Long non-coding rna H19 regulates FOXM1 expression by competitively binding endogenous miR-342-3p in gallbladder cancer. J Exp Clin Cancer Res 2016;35(1):160.
[28] Liu L, Yang J, Zhu X, et al. Long noncoding RNA H19 competitively binds miR-17-5p to regulate YES1 expression in thyroid cancer. FEBS J 2016;283(12):2326–39.
[29] He J, Zhang J, Wang D. Down-regulation of microRNA-216b inhibits IL-1beta-induced chondrocyte injury by up-regulation of Smad3. Biosci Rep 2017;37(2).
[30] Kito N, Endo K, Ikesue M, et al. miRNA profiles of tubular cells: diagnosis of kidney injury. Biomed Res Int 2015;2015:465479.
[31] Xu Z, Bu Y, Chitnis N, et al. miR-216b regulation of c-Jun mediates GADD153/CHOP-dependent apoptosis. Nat Commun 2016;7:11422.
[32] Zhang XX, Deng LH, Chen WW, et al. Circulating microRNA 216 as a marker for the early identification of severe acute pancreatitis. Am J Med Sci 2017;353(2):178–86.
[33] Endo K, Weng H, Kito N, et al. MiR-216a and miR-216b as markers for acute phased pancreatic injury. Biomed Res 2013;34(4):179–88.
[34] Rouse R, Rosenzweig B, Shea K, et al. MicroRNA biomarkers of pancreatic injury in a canine model. Exp Toxicol Pathol 2017;69(1):33–43.
[35] Joshi S, Wang W, Peck AB, et al. Activation of the NLRP3 inflammasome in association with calcium oxalate crystal induced reactive oxygen species in kidneys. J Urol 2015;193(5):1684–91.

Please cite this article as: H. Liu et al., H19 promote calcium oxalate nephrocalcinosis-induced renal tubular epithelial cell injury via a ceRNA pathway, EBioMedicine (2019), https://doi.org/10.1016/j.ebiom.2019.10.059